An Engineered PQQ-Dependent Alcohol Dehydrogenase for the Oxidation of 5-(Hydroxymethyl)furoic Acid

Matthias Wehrmann[a‡], Eslam M. Elsayed[b‡], Sebastian Köbbing[c], Laura Bendz[a], Alexander Lepak[b,d], Johannes Schwabe[b], Nick Wierckx[c,e], Gert Bange[b*], Janosch Klebensberger[a*].

[a]University of Stuttgart, Institute of Biochemistry and Technical Biochemistry, 70569 Stuttgart, Germany

[b]Philipps-University Marburg, SYNMIKRO Research Center and Department of Chemistry, 35043 Marburg, Germany

[c]RWTH Aachen University, Institute of Applied Microbiology-iAMB, 52074 Aachen, Germany

[d]Max Planck Institute for Terrestrial Microbiology, 35043 Marburg, Germany

[e]Forschungszentrum Jülich, Institute of Bio- and Geosciences IBG-1: Biotechnology,52425 Jülich, Germany

KEYWORDS: *protein engineering, lanthanides, HMFA oxidation, biocatalysis, pyrroloquinoline quinone, periplasm, alcohol dehydrogenases, Pseudomonas putida*

Author copy of ACS Catal. 2020, 10, 14, 7836–7842 https://doi.org/10.1021/acscatal.0c01789

ABSTRACT: Furan-2,5-dicarboxylic acid (FDCA) is a bio-based platform chemical with the potential to replace terephthalic acid in the production of polymers. A critical step for enzymatic and whole-cell FDCA production from 5-(hydroxymethyl)furfural (HMF) is the transformation of 5-(hydroxymethyl)furoic acid (HMFA) into 5-formylfuroic acid (FFA). Here, we establish periplasmic pyrroloquinoline quinone (PQQ)-dependent alcohol dehydrogenases (ADH) as biocatalytic tools for the oxidation of HMF and HMFA and further identify the "lid loop" of the substrate channel as a promising target for future engineering steps towards a fully periplasmic oxidation pathway to FDCA.

In 2019, the worldwide plastic production was about 360 million metric tons with over 98 percent of it originating from fossil carbon sources.[1] Carbon dioxide emissions from plastic production and incineration strongly contribute to global warming and climate change. Thus, transitioning towards a bio-based production of plastics based on renewable feedstock and using less energy demanding production processes are essential steps to reach the goal of net-zero greenhouse gas emissions by 2050.[2]

Furan-2,5-dicarboxylic acid (FDCA) is a promising plant-derived platform chemical, which could replace terephthalic acid for the production of polyethylene terephthalate and other polymers.[3,4] FDCA can be synthesized by the oxidation of 5-(hydroxymethyl)furfural (HMF), which itself is easily accessible from lignocellulose, the most abundant biomass on earth.[4,5] As today's chemical synthesis of FDCA typically is highly energy-demanding due to metal catalysts operating at high temperature and pressure, more sustainable routes are sought after.[6] Consequently, various bio-catalytic routes to FDCA have been presented.[7–14] These routes start with an oxidation step of HMF leading either to 5-(hydroxymethyl)furoic acid (HMFA) or 5-(formyl)furfural (FFF) followed by a second oxidation step towards 5-formylfuroic acid (FFA), before finally being oxidized into FDCA (**Fig. 1A**). To the best of our knowledge, one of these routes that employs *Pseudomonas putida* as biocatalyst has recently been established for industrial production.[15–17] In *P. putida*, as well as in many other organisms, furanic aldehydes are rapidly oxidized by native enzymes.[18,19] In contrast, the oxidation of HMFA cannot be performed by cells of the *P. putida* wildtpye[12,18,20] or other strains that have been used to produce HMFA from HMF, such as *Gluconobacter oxydans*[21] or *Comamonas testosteroni*[22]. For FDCA production, the oxidation of HMFA to FFA is crucial and requires the specific HMF oxidase HmfH. Different variants of this enzyme have been heterologously expressed in the cytoplasm of *P. putida* to enable the production of >80 g l^{-1}.[10,12,14,18,23] However, the use of oxidases in whole-cell biotransformations is generally problematic for two reasons: *i.* they require equimolar amounts of molecular oxygen, which is a limiting factor in high-density cultures,[24] and *ii.* the associated cytoplasmic formation of equimolar amounts of cytotoxic hydrogen peroxide as a side product.[25] Although *P. putida* as a microbial catalyst has a high tolerance towards such stresses, the stress response is energy-demanding[26] and thus reduces the overall yield of the process[18].

Pyrroloquinoline quinone (PQQ)-dependent alcohol dehydrogenases (ADHs) could overcome the abovementioned drawbacks as they are functional in the periplasmic space and do not form hydrogen peroxide as co-product. PQQ-ADHs are a class of enzymes that rely on calcium or lanthanide ions as well as PQQ as cofactors to oxidize a

broad spectrum of alcohol and aldehyde substrates.[27–30] They transfer the electrons derived from the oxidation reaction *via c*-type cytochromes to the cytochrome *c* oxidase complex.[31–34] Subsequently, the cytochrome c oxidase efficiently uses four electrons (the equivalent of two substrate oxidation steps) to reduce one molecule of O_2 and additionally generates a source of electrochemical energy in form of the proton motif force.[35] In a whole-cell process this not only provides energy to fulfill maintenance demand[36], it also halves the consumption of oxygen compared to oxidases due to the stoichiometry of this transfer.

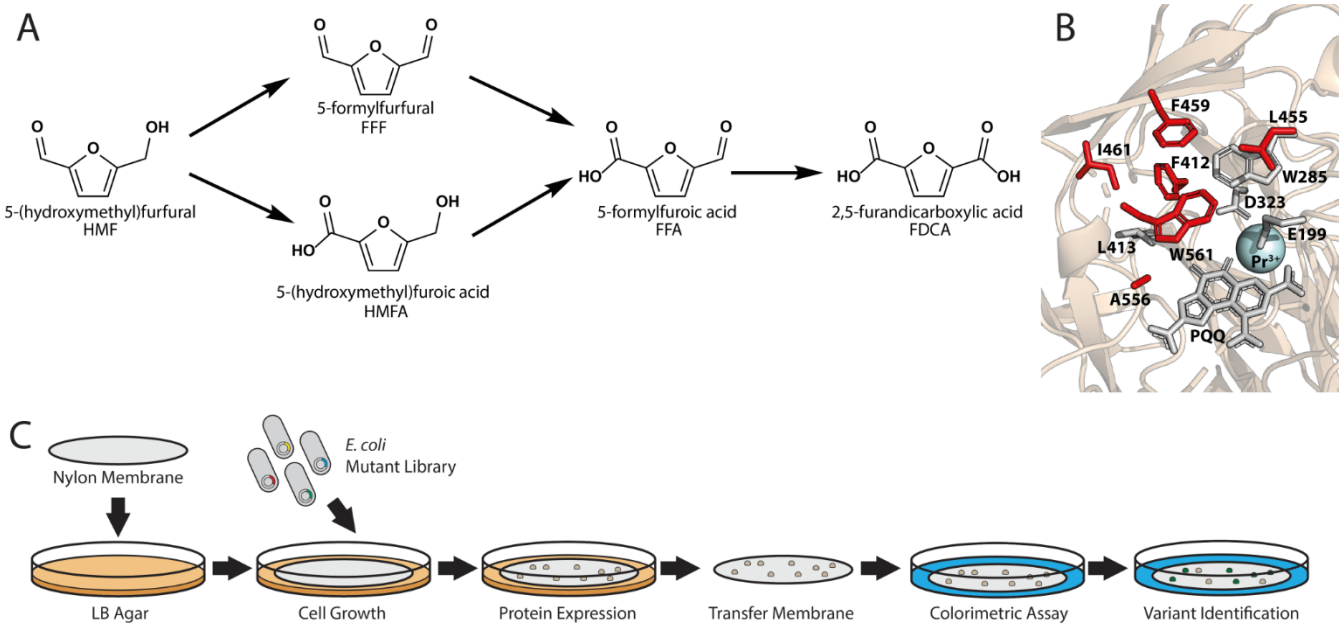

Figure 1: (A) Schematic representation of the oxidation pathways from HMF to FDCA. HMF is either oxidized at the aldehyde group to yield HMFA or at the alcohol group to yield FFA. Upon further oxidation both routes proceed via FFA to FDCA. (B) View of the active site of PedH with PQQ cofactor as well as active site residues that were not included in mutant libraries shown as grey sticks. Residues that were selected for combinatorial random mutagenesis are depicted as red sticks. Pr^{3+} metal cofactor is displayed as blue sphere. (C) Schematic representation of solid phase screening assay. Nylon membranes loaded on LB agar plates were inoculated with *E. coli* cells expressing PedH variants. After growth and protein production, membranes were transferred into colored reaction solution and colonies expressing active variants were identified by surrounding white halo.

Alternatively, also bioelectrochemical systems using PQQ-dependent enzymes, either based on *P. putida* cells or as isolated entities, have been described that can operate even in the absence of molecular oxygen.[37–39]

PQQ-ADHs catalyze the oxidation in an irreversible fashion, leading to unhindered accumulation of the products outside of the cells. Their periplasmic localization would avoid the rate-limiting transport across the cytoplasmic membrane and the associated need for co-expression of the hmfT1 transporter in a whole-cell biotransformation.[15,18] In addition, the cytoplasmic accumulation of furanic aldehydes, which are known for their strong bactericidal properties, could be reduced.[40,41] Lastly, PQQ-ADHs can readily be engineered for increased stability at high temperatures as well as in the presence of organic solvents.[42]

Based on these characteristics, we propose that a biocatalytic route based on PQQ-ADHs would be highly beneficial for the production of FDCA. In the present study, we describe the first and crucial step for a successful realization of such a pathway by engineering a lanthanide-dependent PQQ-ADH from *Pseudomonas putida* KT2440 (PedH) for oxidation of the pathway intermediates HMF and HMFA (**Fig. 1A**).

Initial experiments demonstrated that purified PedH exhibits no enzymatic activity towards HMFA (data not shown). However, marginal activity with HMF (0.13 ± 0.02 U mg^{-1}) was observed. In order to expand the substrate specificity towards the oxidation of HMFA to FFA – a key reaction within the biocatalytic route towards FDCA production – a set of 12 small focused mutant libraries was generated (**Fig. 1B**, **Table S1**). Each mutant library consisted of a pair of NNK-randomized active site positions in order to increase the chances to identify potentially synergistic combinations of mutations.[43] To reduce the creation of inactive variants, no active side residues that are directly involved in the catalytic mechanism were included.[44] To further reduce the screening effort, two additional constraints based on structure-sequence relationship information were applied. These were derived from a 3DM-database consisting of >1300 sequences of PQQ-ADHs that show structural similarity to PedH.[45]Firstly, no positions of low sequence variability in the 3DM database were included. Secondly, only residues with a high correlation score in the 3DM database (**Table S2**), meaning that two positions show a high degree of natural co-evolution,[46] were chosen for combinatorial NNK mutagenesis.

Table 1: Specific enzyme activities of purified PedH as well as variants F412I/W561S, F412I/W561Q, F412V/W561A with 10 mM HMFA as substrate. Values represent the average of three individual measurements with corresponding standard deviation. Activities below detection limit are indicated (n. d.).

Variant	Specific activity [U mg^{-1}]
PedH	n. d.
F412I/W561S	0.12 ± 0.02
F412I/W561Q	0.35 ± 0.01
F412V/W561A	1.04 ± 0.05

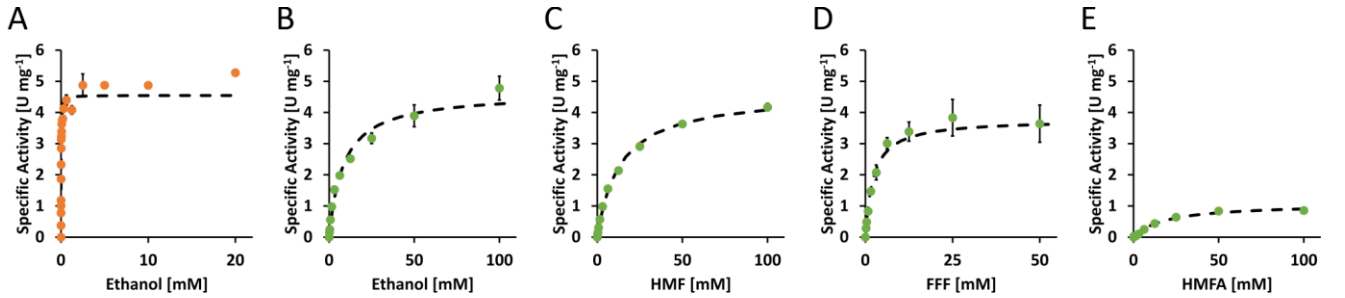

F

PedH

Substrate	k_{cat} [s^{-1}]	K_M [mM]	k_{cat}/K_M [mM^{-1} s^{-1}]
Ethanol	5.0 ± 0.1	0.014 ± 0.001	356 ± 37
HMF	n.d.	n.d.	n.d.
FFF	n.d.	n.d.	n.d.
HMFA	n.d.	n.d.	n.d.

G

PedH$^{F412V/W561A}$

Substrate	k_{cat} [s^{-1}]	K_M [mM]	k_{cat}/K_M [mM^{-1} s^{-1}]
Ethanol	5.1 ± 0.2	8.4 ± 1.0	0.60 ± 0.08
HMF	5.1 ± 0.1	13.3 ± 0.8	0.38 ± 0.03
FFF	4.1 ± 0.3	2.3 ± 0.6	1.81 ± 0.45
HMFA	1.2 ± 0.1	18.8 ± 2.6	0.06 ± 0.01

Figure 2: Kinetic parameter determination. (A to E) Michaelis-Menten plot showing the specific enzyme activities of PedH wildtype (A) and PedH$^{F412V/W561A}$ variant (B to E) with different concentrations of ethanol (A and B), HMF (C), FFF (D) or HMFA (E). Kinetic parameters of PedH (F) and PedH$^{F412V/W561A}$ (G) derived by fitting specific enzyme activities at different substrates to the Michaelis-Menten model of single-substrate enzyme kinetics.

To screen these combinatorial libraries, we developed a colony screen, based on a previously established whole-cell assay (**Fig. 1C**).[42] For this, *E. coli* cells transformed with the combinatorial libraries grew on nylon membranes placed on LB agar plates. The transfer of the membrane onto rhamnose-containing LB agar subsequently induced plasmid-borne protein production. After incubation of the membranes in a colorimetric assay solution, colonies with enzymatic activity towards HMFA were identified by a white halo (**Fig. 1C**).

In the initial screening more than 30.000 clones were tested. As a result, 15 clones showed apparent enzymatic activity towards HMFA. Re-evaluation of the novel enzymatic activity and subsequent sequencing revealed three different variants with activity towards HMFA, namely PedH$^{F412I/W561S}$, PedH$^{F412V/W561A}$ and PedH$^{F412I/W561Q}$ (**Table 1**). To exclude potential host specific effects, activities for all variants were evaluated using enzymes purified by affinity chromatography (IMAC). The variants PedH$^{F412I/W561S}$ and PedH$^{F412I/W561Q}$ showed a specific activity with HMFA of 0.12 ± 0.02 U mg^{-1} and 0.35 ± 0.01 U mg^{-1}, respectively. PedH$^{F412V/W561A}$ exhibited by far the highest specific activity of 1.04 ± 0.05 U mg^{-1}. Notably, all variants are combinatorial mutants derived from the same mutant library PedH$^{F412X/W561X}$ suggesting that a single point mutation at position F412 or W561 is not sufficient to alter the substrate specificity towards HMFA.

To identify the reaction product, biotransformations using purified enzymes and the artificial electron mediator/terminal acceptor pair PMS/DCPIP were performed (**Table 2**). While no product formation was detected with PedH or in control experiments without enzyme addition, FFA was identified as the single reaction product (1.40 ± 0.11 mM in 24 h) in conversions using PedH$^{F412V/W561A}$. Further oxidation to FDCA was not detected.

To verify the screening results and gain mechanistic insights into the novel activity towards HMFA, we purified PedH and its F412V/W561A variant using His-affinity- followed by size-exclusion chromatography. Kinetic parameters of PedH and PedH$^{F412V/W561A}$ were derived from specific activities determined under a slightly modified protocol compared to the initial screens to reach saturating substrate concentrations (≥ 50 mM HMFA). Under these conditions, PedH$^{F412V/W561A}$ exhibited kinetic values with HMFA (**Fig. 2E, G**) that were in a similar range as the reported kinetic constants of the only characterized proteins with activity towards HMFA, namely the 5-(hydroxymethyl)furfural oxidase HmfO of *Methylovorus* sp. strain MP688 (k_{cat} = 8.5 s^{-1}, K_M = 73 mM, k_{cat}/K_M = 0.12 mM^{-1} s^{-1}) and the aryl-alcohol oxidase AAO of *Pleurotus eryngii* (k_{cat} = n. d., K_M = n. d., k_{cat}/K_M = 0.017 ± 0.002 mM^{-1} s^{-1}).[8,47] Consistent with our initial observations, PedH showed no activity with HMFA (**Figs. 2E**). Additionally, both PedH and PedH$^{F412V/W561A}$ oxidized ethanol (**Figs. 2A, B**). However, PedH$^{F412V/W561A}$ exhibited an approximately 520-fold higher

K_M value than PedH, while the maximal velocity appeared to be unchanged (**Figs. 2F, G**).

Table 2: Biotransformations of HMFA using purified PedH$^{F412V/W561A}$ and an enzyme free control with PMS/DCPIP as artificial electron acceptor pair. Samples were taken at several time points after substrate addition. Values represent average of two individual measurements with corresponding standard deviation. Enzymatic reaction without detectable product formation are indicated (n. d.).

Time [h]	FFA [mM]		
	Control	PedH	PedH$^{F412V/W561A}$
0	n. d.	n. d.	0.28 ± 0.01
1	n. d.	n. d.	1.24 ± 0.15
24	n. d.	n. d.	1.40 ± 0.11

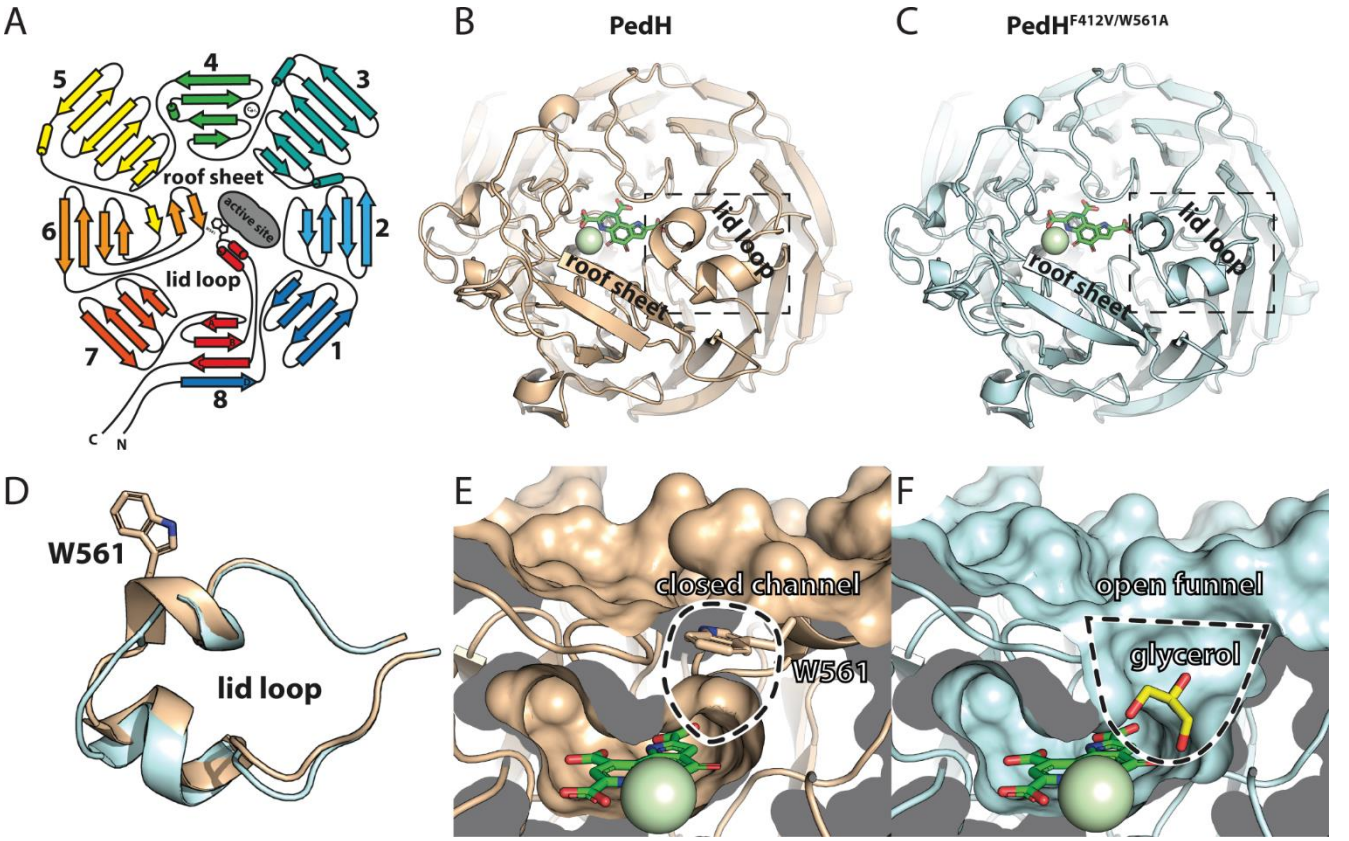

Figure 3: (A) Schematic representation of the β-propeller and position of the active site. Top view of PedH wildtype (B) and PedH$^{F412V/W561A}$ (C) showing the position of the roof sheet and the lid loop. (D) Overlay of the lid loop in PedH wildtype (wheat) PedH$^{F412V/W561A}$ (blue) and relative position of W561. Cut-away of the active site in PedH wildtype (E) and PedH$^{F412V/W561A}$ variant (F). Glycerol as the substrate mimic in the active site of the PedH$^{F412V/W561A}$ variant is depicted in yellow.

This suggests that the oxidative capability of the PedH$^{F412V/W561A}$ variant is unaffected by the amino acid changes, and only the substrate binding is modulated.

In addition to HMFA, PedH$^{F412V/W561A}$ also oxidized HMF and FFF. In comparison to HMFA, the maximal velocity with HMF and FFF as substrate was about 5-fold and 4-fold higher, respectively.(**Figs. 2C, D**, **E**, **G**). This might be caused by the electron withdrawing nature of the carboxyl group on the conjugated ring system in HMFA. Notably, the PedH wildtype showed no activity with FFF. In contrast to our initial findings, PedH also displayed no activity with HMF as substrate. However, this discrepancy can most likely be explained by the change of the enzymatic assay conditions, which caused overall lower specific activities compared to the initial screening conditions. Enzymatic assays with PedH$^{F412V/W561A}$ confirmed that FFA does not serve as a substrate under these conditions as even with substrate concentrations as high as 100 mM, no enzyme activity could be detected. This sheds new light on the previously perceived importance of PQQ-ADHs in HMF oxidation to FDCA.[18]

Taken together, these findings show that the PedH$^{F412V/W561A}$ variant is capable of not only oxidizing HMFA but also HMF and FFF, while it is not able to oxidize FFA. Aldehyde oxidation by PQQ-ADHs is believed to proceed via the hydrated aldehyde and the stability and/or formation of these gem-diols are therefore crucial for activity.[44]

Gem-diol formation of FFA in aqueous solution is dramatically lower in comparison to FFF.[7,48] Additionally, the carboxylic group of HMFA negatively influences both the substrate affinity and the catalytic activity. The lack of activity towards FFA can therefore most likely be explained by a combination of the low effective concentration of the

diol substrate, the decreased activity due to the electron withdrawing nature of the carboxyl group and the reduced substrate affinity of the variant towards carboxylated furan compounds. Future engineering efforts would consequently need to improve substrate binding to enable the conversion of this furan aldehyde.

To interrogate the molecular basis of these findings, we determined the structures of PedH and PedH$^{F412V/W561A}$ bound to PQQ and praseodymium to resolutions of 1.7 Å and 1.6 Å, respectively (**Table S3**). The crystal structures show the typical beta propeller fold consisting of 8 four-stranded β-blades (W1 to W8) as the core structural element with three additional strands inserted after W5 (named: "roof sheet") (**Fig. 3A**). Two small α-helices are inserted between the strands B and C of W8 (named: "lid loop"). The active site containing the PQQ cofactor and praseodymium ion localizes in a hydrophobic cradle close to the surface of the β-propeller. Here, PQQ is coordinated by Q87, I135, R137, S181, R350, L413, N417, W418, W493 (**Fig. S1A**). The side chains of W263 and vicinal disulfide bond between C131 and C132 provide additional stacking interactions with PQQ (**Fig. S1B**). The praseodymium ion coordination is highly conserved and achieved by the amino acid side chains of E199, N281, D323, D325 and the O5 and O7A atoms of the PQQ cofactor (**Fig. S1A**). Structural comparison of PedH and PedH$^{F412V/W561A}$ shows that neither the PQQ nor the metal binding environment is changed. However, our comparison also shows significant differences between both structures (**Fig. 3B, C**). Access to the PQQ/praseodymium-containing active site is provided through a substrate channel of about 4 Å in diameter (lined by: F412, L413) and a length of 9 Å (shortest distance from the metal ion to the PedH surface). In PedH, W561 within the "lid loop" restricts this substrate channel reminiscent to a diaphragm and hampers the entrance of bulkier substrates. In PedH$^{F412V/W561A}$, W561 is replaced by alanine, which leads to an opening of the substrate channel. In PedH, F412 lines the inner surface of the substrate channel and serves in positioning the "lid loop" relative to the center of the substrate channel (**Figs. 3D, E, F**).

In the structure of PedH$^{F412V/W561A}$, replacement of F412 with the "smaller" valine not only widens the substrate channel at its bottom, but also leads to a remodeling and repositioning of the "lid loop" including the amino acid positions 559 to 566 effectively moving the loop backbone about 2.5 Å away from the channel entrance (**Figs. 3B, C, D**).

Taken together, our structural analysis shows that the amino acid changes remodel the narrow substrate channel of PedH into a much wider one in PedH$^{F412V/W561A}$, which is not shielded from substrate entry by the "lid-loop". In accordance with these structural changes, we found electron density for a glycerol in the active site of PedH$^{F412V/W561A}$. This molecule might illustrate how the similarly sized HMFA, HMF and FFF easily pass through the widened channel in PedH$^{F412V/W561A}$ compared to the impeded access in the PedH enzyme (compare: **Figs. 3E, F and S2A**). These observations are consistent with the increased activities of PedH$^{F412V/W561A}$ towards HMF and the newly gained activity towards HMFA as well as FFF and further explain the massively increased K_M value of PedH$^{F412V/W561A}$ for ethanol. Additionally, an overlay of the glycerol molecule with HMFA indicates that in an active binding conformation the apolar residue L560 of the lid-loop as well as L455 and the phenol rings of W285 and F459 point towards the negatively charged carboxyl group of HMFA (**Fig. S2B**). This might not only explain the decreased K_M of PedH$^{F412V/W561A}$ for HMFA in comparison with the uncharged HMF or FFF but might also reveal promising targets for the further engineering of FFA activity.

In conclusion, our work established a novel screening platform for engineered PQQ-ADHs. With this platform, two active site residues that are crucial to expand the substrate scope of PedH towards HMFA were found. The best double mutant exhibits activities similar to known HMFA oxidizing enzymes and could serve as an alternative to currently employed oxidases.

Structural analysis of the variant revealed significant changes to the geometry and composition of several active site and substrate channel features and suggests the "lid loop" as attractive target for further engineering of this enzyme class. By targeting the identified residues, additional variants with a lower K_M, or increased and/or *de novo* activities towards other pathway intermediates could be engineered. With these, a whole-cell biocatalyst with a completely periplasmic production route from HMF to FDCA can be envisioned. Such a route would avoid the intracellular formation of toxic by-products or intermediates such as hydrogen peroxide and furan aldehydes. Consequently, the stress-associated maintenance for the cell would be reduced, instead efficient channeling of electrons from the oxidation reaction into the cellular energy metabolism. In general, our study shows that PQQ-dependent ADH enzymes can be engineered into useful tools for biocatalysis and paves the way for their application in bio-based plastic production.

ASSOCIATED CONTENT

Data Availability. Coordinates and structure factors have been deposited at the Protein Data Bank (PDB) under the accession codes: XXX (wildtype PedH) and YYY (PedH$^{F412V/W561A}$).

Supporting Information. Experimental details. Mutant library composition. Crystallographic data collection and refinement statistics. Structure of PQQ coordination in the active site of PedH. This information is available free of charge on the ACS Publications website.

AUTHOR INFORMATION

Corresponding Author

* Correspondence should be addressed to janosch.klebensberger@itb.uni-stuttgart.de and gert.bange@synmikro.uni-marburg.de.

Author Contributions

J.K. and M.W. conceptualized the work and wrote the original draft of the manuscript. All authors contributed to writing, reviewing and editing of the manuscript as well as data analysis and visualization. J.K. and G.B. acquired the financial support

for the project and J.K., G.B. and N.W. supervised the work. M.W., E.M.E., S.K., L.B., A.L., J.S. conducted the research. / ‡These authors contributed equally.

Funding Sources

The work of M.W. and J.K. was supported by an individual research grant from the Deutsche Forschungsgemeinschaft (KL 2340/2-1). We thank the Jameel Education Foundation Scholarship Fund Programme for the financial support of E.M.E.. S.K. acknowledges funding from the European Union's Horizon 2020 Research and Innovation Programme under Grant Agreement No. 633962 for the project P4SB. N.W. acknowledges funding from the German Federal Ministry of Education and Research (BMBF, FKZ 031B0852A).

Notes

The authors declare no competing financial interest.

ACKNOWLEDGMENT

We thank the LOEWE initiative of the state of Hesse for excellent support (to G.B.). We acknowledge beamline support from the Deutsche Elektronen Synchrotron (DESY, Hamburg). Harald Ruijssenaars (Corbion Biochem BV) is kindly acknowledged for providing analytical standards of HMF derivatives and Bernhard Hauer and Lars M. Blank for their continuous support.

ABBREVIATIONS

PQQ, pyrroloquinoline quinone; PQQ-ADH, pyrroloquinoline quinone dependent alcohol dehydrogenase; REE, rare earth element; FDCA, furan-2,5-dicarboxylic acid; HMFA, 5-(hydroxymethyl)furoic acid; FFF, 5-(formyl)furfural; HMF, 5-(hydroxymethyl)furfural.

REFERENCES

(1) European Bioplastics www.european-bioplastics.org.

(2) European Parliament [Press Release]. The European Parliament Declares Climate Emergency. *European Parliament*. 2019.

(3) Werpy, T.; Petersen, G. *Top Value Added Chemicals from Biomass: Volume I -- Results of Screening for Potential Candidates from Sugars and Synthesis Gas*; Golden, CO (United States), 2004; Vol. II. https://doi.org/10.2172/15008859.

(4) Yuan, H.; Liu, H.; Du, J.; Liu, K.; Wang, T.; Liu, L. Biocatalytic Production of 2,5-Furandicarboxylic Acid: Recent Advances and Future Perspectives. *Appl. Microbiol. Biotechnol.* **2020**, *104* (2), 527–543. https://doi.org/10.1007/s00253-019-10272-9.

(5) Rosatella, A. A.; Simeonov, S. P.; Frade, R. F. M.; Afonso, C. A. M. 5-Hydroxymethylfurfural (HMF) as a Building Block Platform: Biological Properties, Synthesis and Synthetic Applications. *Green Chem.* **2011**, *13* (4), 754–793. https://doi.org/10.1039/cogc00401d.

(6) Delidovich, I.; Hausoul, P. J. C.; Deng, L.; Pfützenreuter, R.; Rose, M.; Palkovits, R. Alternative Monomers Based on Lignocellulose and Their Use for Polymer Production. *Chem. Rev.* **2016**, *116* (3), 1540–1599. https://doi.org/10.1021/acs.chemrev.5b00354.

(7) Dijkman, W. P.; Groothuis, D. E.; Fraaije, M. W. Enzyme-Catalyzed Oxidation of 5-Hydroxymethylfurfural to Furan-2,5-Dicarboxylic Acid. *Angew. Chemie - Int. Ed.* **2014**, *53* (25), 6515–6518. https://doi.org/10.1002/anie.201402904.

(8) Carro, J.; Ferreira, P.; Rodríguez, L.; Prieto, A.; Serrano, A.; Balcells, B.; Ardá, A.; Jiménez-Barbero, J.; Gutiérrez, A.; Ullrich, R.; Hofrichter, M.; Martínez, A. T. 5-Hydroxymethylfurfural Conversion By Fungal Aryl-Alcohol Oxidase and Unspecific Peroxygenase. *FEBS J.* **2015**, *282* (16), 3218–3229. https://doi.org/10.1111/febs.13177.

(9) McKenna, S. M.; Leimkühler, S.; Herter, S.; Turner, N. J.; Carnell, A. J. Enzyme Cascade Reactions: Synthesis of Furandicarboxylic Acid (FDCA) and Carboxylic Acids Using Oxidases in Tandem. *Green Chem.* **2015**, *17* (6), 3271–3275. https://doi.org/10.1039/c5gc00707k.

(10) Koopman, F.; Wierckx, N.; de Winde, J. H.; Ruijssenaars, H. J. Efficient Whole-Cell Biotransformation of 5-(Hydroxymethyl)Furfural into FDCA, 2,5-Furandicarboxylic Acid. *Bioresour. Technol.* **2010**, *101* (16), 6291–6296. https://doi.org/10.1016/j.biortech.2010.03.050.

(11) Yuan, H.; Li, J.; Shin, H. dong; Du, G.; Chen, J.; Shi, Z.; Liu, L. Improved Production of 2,5-Furandicarboxylic Acid by Overexpression of 5-Hydroxymethylfurfural Oxidase and 5-Hydroxymethylfurfural/Furfural Oxidoreductase in Raoultella Ornithinolytica BF60. *Bioresour. Technol.* **2018**, *247*, 1184–1188. https://doi.org/10.1016/j.biortech.2017.08.166.

(12) Hsu, C.-T.; Kuo, Y.-C.; Liu, Y.-C.; Tsai, S.-L. Green Conversion of 5-Hydroxymethylfurfural to Furan-2,5-Dicarboxylic Acid by Heterogeneous Expression of 5-Hydroxymethylfurfural Oxidase in Pseudomonas Putida S12. *Microb. Biotechnol.* **2020**, *0* (0), 1–9. https://doi.org/10.1111/1751-7915.13564.

(13) Dijkman, W. P.; Binda, C.; Fraaije, M. W.; Mattevi, A. Structure-Based Enzyme Tailoring of 5-Hydroxymethylfurfural Oxidase. *ACS Catal.* **2015**, *5* (3), 1833–1839. https://doi.org/10.1021/acscatal.5b00031.

(14) Pham, N. N.; Chen, C.; Li, H.; Nguyen, M. T. T.; Nguyen, P. K. P.; Tsai, S.; Chou, J.; Ramli, T. C.; Hu, Y. Engineering Stable Pseudomonas Putida S12 by CRISPR for 2,5-Furandicarboxylic Acid (FDCA) Production. *ACS Synth. Biol.* **2020**, *9* (5), 1138–1149. https://doi.org/10.1021/acssynbio.0c00006.

(15) Wierckx, N.; Elink Schuurman, T. D.; Kuijper, S.; Ruijssenaars, H. J. Genetically Modified Cell and Process for Use of Said Cell. WO2012064195A2, 2012.

(16) Ruijssenaars, H. J.; Wierckx, N.; Koopman, F.; Straathof, A.; De Winde, J. H. Polypeptides Having Oxidoreductase Activity And Their Uses. WO2011026913, 2010.

(17) Sajid, M.; Zhao, X.; Liu, D. Production of 2,5-Furandicarboxylic Acid (FDCA) from 5-Hydroxymethylfurfural (HMF): Recent Progress Focusing on the Chemical-Catalytic Routes. *Green Chem.* **2018**, *20* (24), 5427–5453. https://doi.org/10.1039/C8GC02680G.

(18) Wierckx, N.; Elink Schuurman, T. D.; Blank, L. M.; Ruijssenaars, H. J. Whole-Cell Biocatalytic Production of 2,5-Furandicarboxylic Acid. In *Molecular Microbiology*; Kamm, B., Ed.; Microbiology Monographs; Springer Berlin Heidelberg: Berlin, Heidelberg, 2015; Vol. 26, pp 207–223. https://doi.org/10.1007/978-3-662-45209-7_8.

(19) Hu, L.; He, A.; Liu, X.; Xia, J.; Xu, J.; Zhou, S.; Xu, J. Biocatalytic Transformation of 5-Hydroxymethylfurfural into High-Value Derivatives: Recent Advances and Future Aspects. *ACS Sustain. Chem. Eng.* **2018**, *6* (12), 15915–15935. https://doi.org/10.1021/acssuschemeng.8b04356.

(20) Xu, Q.; Zheng, Z.; Zou, L.; Zhang, C.; Yang, F.; Zhou, K.; Ouyang, J. A Versatile Pseudomonas Putida KT2440 with New Ability: Selective Oxidation of 5-Hydroxymethylfurfural to 5-Hydroxymethyl-2-Furancarboxylic Acid. *Bioprocess Biosyst. Eng.* **2020**, *43* (1), 67–73. https://doi.org/10.1007/s00449-019-02205-7.

(21) Sayed, M.; Pyo, S.-H.; Rehnberg, N.; Hatti-Kaul, R. Selective Oxidation of 5-Hydroxymethylfurfural to 5-Hydroxymethyl-2-Furancarboxylic Acid Using Gluconobacter Oxydans. *ACS Sustain. Chem. Eng.* **2019**, *7* (4), 4406–4413. https://doi.org/10.1021/acssuschemeng.8b06327.

(22) Zhang, X. Y.; Zong, M. H.; Li, N. Whole-Cell Biocatalytic Selective Oxidation of 5-Hydroxymethylfurfural to 5-Hydroxymethyl-2-Furancarboxylic Acid. *Green Chem.* **2017**, *19* (19), 4544–4551. https://doi.org/10.1039/c7gc01751k.

(23) Koopman, F.; Wierckx, N.; De Winde, J. H.; Ruijssenaars, H. J. Identification and Characterization of the Furfural and 5-(Hydroxymethyl)Furfural Degradation Pathways of Cupriavidus Basilensis HMF14. *Proc. Natl. Acad. Sci.* **2010**, *107* (11), 4919–4924. https://doi.org/10.1073/pnas.0913039107.

(24) Baldwin, C. V. F.; Woodley, J. On Oxygen Limitation in a Whole Cell Biocatalytic Baeyer–Villiger Oxidation Process. *Biotechnol. Bioeng.* **2006**, *95* (3), 362–369. https://doi.org/10.1002/bit.20869.

(25) Linley, E.; Denyer, S. P.; McDonnell, G.; Simons, C.; Maillard, J.-Y. Use of Hydrogen Peroxide as a Biocide: New Consideration of Its Mechanisms of Biocidal Action. *J. Antimicrob. Chemother.* **2012**, *67* (7), 1589–1596. https://doi.org/10.1093/jac/dks129.

(26) Kim, J.; Park, W. Oxidative Stress Response in Pseudomonas Putida. *Appl. Microbiol. Biotechnol.* **2014**, *98* (16), 6933–6946. https://doi.org/10.1007/s00253-014-5883-4.

(27) Keltjens, J. T.; Pol, A.; Reimann, J.; Op den Camp, H. J. M. PQQ-Dependent Methanol Dehydrogenases: Rare-Earth Elements Make a Difference. *Appl. Microbiol. Biotechnol.* **2014**, *98* (14), 6163–6183. https://doi.org/10.1007/s00253-014-5766-8.

(28) Wehrmann, M.; Billard, P.; Martin-Meriadec, A.; Zegeye, A.; Klebensberger, J. Functional Role of Lanthanides in Enzymatic Activity and Transcriptional Regulation of Pyrroloquinoline Quinone-Dependent Alcohol Dehydrogenases in Pseudomonas Putida KT2440. *MBio* **2017**, *8* (3), e00570-17. https://doi.org/10.1128/mBio.00570-17.

(29) Good, N. M.; Vu, H. N.; Suriano, C. J.; Subuyuj, G. A.; Skovran, E.; Martinez-Gomez, N. C. Pyrroloquinoline Quinone Ethanol Dehydrogenase in Methylobacterium Extorquens AM1 Extends Lanthanide-Dependent Metabolism to Multicarbon Substrates. *J. Bacteriol.* **2016**, *198* (22), 3109–3118. https://doi.org/10.1128/JB.00478-16.

(30) Jahn, B.; Pol, A.; Lumpe, H.; Barends, T. R. M.; Dietl, A.; Hogendoorn, C.; Op den Camp, H. J. M.; Daumann, L. Similar but Not the Same: First Kinetic and Structural Analyses of a Methanol Dehydrogenase Containing a Europium Ion in the Active Site. *ChemBioChem* **2018**, *19* (11), 1147–1153. https://doi.org/10.1002/cbic.201800130.

(31) Zheng, Y.; Huang, J.; Zhao, F.; Chistoserdova, L. Physiological Effect of XoxG(4) on Lanthanide-Dependent Methanotrophy. *MBio* **2018**, *9* (2), e02430-17. https://doi.org/10.1128/mBio.02430-17.

(32) Versantvoort, W.; Pol, A.; Daumann, L. J.; Larrabee, J. A.; Strayer, A. H.; Jetten, M. S. M.; van Niftrik, L.; Reimann, J.; Op den Camp, H. J. M. Characterization of a Novel Cytochrome c as the Electron Acceptor of XoxF-MDH in the Thermoacidophilic Methanotroph Methylacidiphilum Fumariolicum SolV. *Biochim. Biophys. Acta - Proteins Proteomics* **2019**, *1867* (6), 595–603. https://doi.org/10.1016/j.bbapap.2019.04.001.

(33) Schobert, M.; Görisch, H. Cytochrome C550 Is an Essential Component of the Quinoprotein Ethanol Oxidation System in Pseudomonas Aeruginosa: Cloning and Sequencing of the Genes Encoding Cytochrome C550 and an Adjacent Acetaldehyde Dehydrogenase. *Microbiology* **1999**, *145* (2), 471–481. https://doi.org/10.1099/13500872-145-2-471.

(34) Goodwin, P. M.; Anthony, C. The Biochemistry, Physiology and Genetics of PQQ and PQQ-Containing Enzymes. In *Advances in Microbial Physiology*; 1998; Vol. 40, pp 1–80. https://doi.org/10.1016/S0065-2911(08)60129-0.

(35) García-Horsman, J. A.; Barquera, B.; Rumbley, J.; Ma, J.; Gennis, R. B. The Superfamily of Heme-Copper Respiratory Oxidases. *J. Bacteriol.* **1994**, *176* (18), 5587–5600. https://doi.org/10.1128/jb.176.18.5587-5600.1994.

(36) Hardy, G. Energy Conservation by Pyrroloquinoline Quinol-Linked Xylose Oxidation in Pseudomonas Putida NCTC 10936 during Carbon-Limited Growth in Chemostat Culture. *FEMS Microbiol. Lett.* **1993**, *107* (1), 107–110. https://doi.org/10.1016/0378-1097(93)90362-6.

(37) Yu, S.; Lai, B.; Plan, M. R.; Hodson, M. P.; Lestari, E. A.; Song, H.; Krömer, J. Improved Performance of Pseudomonas Putida in a Bioelectrochemical System through Overexpression of Periplasmic Glucose Dehydrogenase. *Biotechnol. Bioeng.* **2018**, *115* (1), 145–155. https://doi.org/10.1002/bit.26433.

(38) Lai, B.; Yu, S.; Bernhardt, P. V.; Rabaey, K.; Virdis, B.; Krömer, J. Anoxic Metabolism and Biochemical Production in Pseudomonas Putida F1 Driven by a Bioelectrochemical System. *Biotechnol. Biofuels* **2016**, *9* (1), 39. https://doi.org/10.1186/s13068-016-0452-y.

(39) Takeda, K.; Matsumura, H.; Ishida, T.; Samejima, M.; Igarashi, K.; Nakamura, N.; Ohno, H. The Two-Step Electrochemical Oxidation of Alcohols Using a Novel Recombinant PQQ Alcohol Dehydrogenase as a Catalyst for a Bioanode. *Bioelectrochemistry* **2013**, *94*, 75–78. https://doi.org/10.1016/j.bioelechem.2013.08.001.

(40) Heer, D.; Sauer, U. Identification of Furfural as a Key Toxin in Lignocellulosic Hydrolysates and Evolution of a Tolerant Yeast Strain. *Microb. Biotechnol.* **2008**, *1* (6), 497–506. https://doi.org/10.1111/j.1751-7915.2008.00050.x.

(41) Zaldivar, J.; Martinez, A.; Ingram, L. O. Effect of Selected Aldehydes on the Growth and Fermentation of EthanologenicEscherichia Coli. *Biotechnol. Bioeng.* **1999**, *65* (1), 24–33. https://doi.org/10.1002/(SICI)1097-0290(19991005)65:1<24::AID-BIT4>3.0.CO;2-2.

(42) Wehrmann, M.; Klebensberger, J. Engineering Thermal Stability and Solvent Tolerance of the Soluble Quinoprotein PedE from Pseudomonas Putida KT2440 with a Heterologous Whole-Cell Screening Approach. *Microb. Biotechnol.* **2018**, *11* (2), 399–408. https://doi.org/10.1111/1751-7915.13036.

(43) Reetz, M. T.; Bocola, M.; Carballeira, J. D.; Zha, D.; Vogel, A. Expanding the Range of Substrate Acceptance of Enzymes: Combinatorial Active-Site Saturation Test. *Angew. Chemie - Int. Ed.* **2005**, *44* (27), 4192–4196. https://doi.org/10.1002/anie.200500767.

(44) Oubrie, A.; Rozeboom, H. J.; Kalk, K. H.; Huizinga, E. G.; Dijkstra, B. W. Crystal Structure of Quinohemoprotein Alcohol Dehydrogenase from Comamonas Testosteroni: Structural Basis for Substrate Oxidation and Electron Transfer. *J. Biol. Chem.* **2002**, *277* (5), 3727–3732. https://doi.org/10.1074/jbc.M109403200.

(45) Kuipers, R.; Joosten, H. J.; van Berkel, W. J. H.; Leferink, N. G. H.; Rooijen, E.; Ittmann, E.; van Zimmeren, F.; Jochens, H.; Bornscheuer, U.; Vriend, G.; Martins dos Santos, V. A. P.; Schaap, P. J. 3DM: Systematic Analysis of Heterogeneous Superfamily Data to Discover Protein Functionalities. *Proteins Struct. Funct. Bioinforma.* **2010**, *78* (9), NA-NA. https://doi.org/10.1002/prot.22725.

(46) Kuipers, R.; Joosten, H. J.; Verwiel, E.; Paans, S.; Akerboom, J.; Van Der Oost, J.; Leferink, N. G. H.; Van Berkel, W. J. H.; Vriend, G.; Schaap, P. J. Correlated Mutation Analyses on Super-Family Alignments Reveal Functionally Important Residues. *Proteins Struct. Funct. Bioinforma.* **2009**, *76* (3), 608–616. https://doi.org/10.1002/prot.22374.

(47) Dijkman, W. P.; Fraaije, M. W. Discovery and Characterization of a 5-Hydroxymethylfurfural Oxidase from Methylovorus Sp. Strain MP688. *Appl. Environ. Microbiol.* **2014**, *80* (3), 1082–1090. https://doi.org/10.1128/AEM.03740-13.

(48) Bell, R. P. The Reversible Hydration of Carbonyl Compounds. In *Acta Crystallographica Section D Biological Crystallography*; 1966; Vol. 60, pp 1–29. https://doi.org/10.1016/S0065-3160(08)60351-2.

GRAPHICAL ABSTRACT

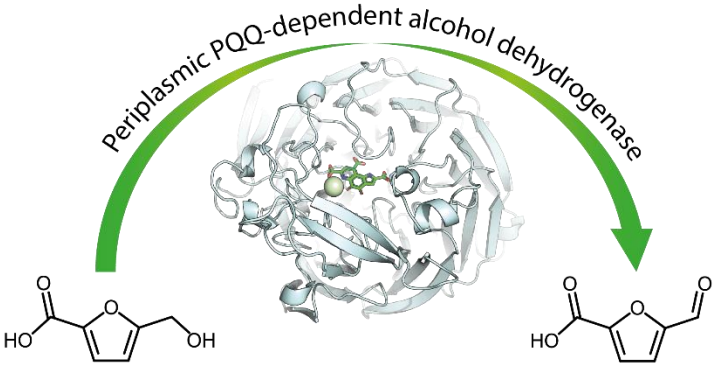

Supporting Information

An Engineered PQQ-Dependent Alcohol Dehydrogenase for the Oxidation of 5-(Hydroxymethyl)furoic Acid

Matthias Wehrmann[a†], Eslam M. Elsayed[b†], Sebastian Köbbing[c], Laura Bendz[a], Alexander Lepak[b,d], Johannes Schwabe[b], Nick Wierckx[c,e], Gert Bange[b*], Janosch Klebensberger[a*]

[a]University of Stuttgart, Institute of Biochemistry and Technical Biochemistry, 70569 Stuttgart, Germany

[b]Philipps-University Marburg, SYNMIKRO Research Center and Department of Chemistry, 35043 Marburg, Germany

[c]RWTH Aachen University, Institute of Applied Microbiology-iAMB, 52074 Aachen, Germany

[d]Max Planck Institute for Terrestrial Microbiology, 35043 Marburg, Germany

[e]Forschungszentrum Jülich, Institute of Bio- and Geosciences IBG-1: Biotechnology, 52425 Jülich, Germany

[†]Authors contributed equally
*Correspondence should be addressed to janosch.klebensberger@itb.uni-stuttgart.de and gert.bange@synmikro.uni-marburg.de

Materials and Methods

Bacterial strains and growth conditions. For cloning and expression *Escherichia coli* Bl21 (DE3) was used and if not stated otherwise, cells were routinely grown in liquid LB medium at 37°C and 180 rpm shaking in a rotary shaker.[1] For plasmid maintenance and selection 40 µg/ml of kanamycin were supplemented to the growth media.

Library construction and evaluation. DNA-fragments of the *pedH* gene containing ends homologous to the SrfI and HindIII digested expression vector pMW10[2] were and NNK randomization at the desired positions (see **Figure 1b**) were synthesized by an external supplier (Synbio Technologies, USA). For library construction the pedMW10 vector was digested using SrfI and HindIII, purified and joined with the NNK-randomized DNA fragments using one-step isothermal assembly.[3] The reaction product was subsequently transformed into *E. coli* BL21(DE3) cells and plated on LB-agar. A minimum of 2500 clones per library were subsequently suspended in LB-medium and stored as glycerol stocks (30% v/v) at -80°C until further usage. To evaluate library quality the plasmids from 56 individual clones were purified and the correctness was verified using Sanger sequencing. As around 20 % of the sequenced clones did not contain the correct insert, the screening size was increased accordingly.

Solid-phase screening assay. The solid phase screening assay to detect PQQ-ADH activity in cell colonies grown on nylon membranes was based on a previously developed screening assay for PQQ-ADHs in liquid cell cultures.[4] In the final protocol 200 µL of a *E. coli* BL21(DE3) cell suspension (OD_{600} = 3 x 10^6) were spread on a nylon membrane (pore size 0.45 µm, GVS Life Sciences) loaded LB_{Kan} agar plate supplemented with 100 µM $PrCl_3$. Upon incubation for 16 h at 37°C protein production was induced by transferring the membranes were transferred onto new LB_{Kan} agar plates supplemented with 100 µM $PrCl_3$, 10 µM PQQ and 0.2% rhamnose. Upon incubation for 24 h at 16°C the membranes were washed placing them for 10 min on a round filter (Rotilabo Type 113A, Carl Roth GmbH) soaked in 3 ml 100 mM Tris buffer (pH 8). Upon drying on cellulose paper for 5 min, the washed membranes were transferred onto a new round filter that was immersed in 3 ml of a colorimetric enzyme activity assay solution (100 mM Tris buffer pH 8, 5 µM PQQ, 5 µM PrCl3, 500 µM phenazine methosulfate, 25 mM imidazole, 30 mM KCN, 10 mM substrate) and incubated in darkness under the hood for 1 – 24 h. Cell colonies producing PQQ-ADHs with activity towards the tested substrate were identified by a white halo.

Library screening. To guarantee with 80% certainty that each variant of the library is tested at least once, at least 1978 colonies (32 [NNK] x 32 [NNK] x 1.2 [correction for vectors without insert] x 1.61 [oversampling factor])[5] per mutant library were screened for activity with 10 mM HMFA using the solid-phase activity assay (see solid-phase screening assay). Colonies that showed activity with HMFA were isolated on LB_{Kan} agar plates and reevaluated in triplicates in a second round of screening. Therefore one colony per identified clone was resuspended in 20 µL H_2O and 3x 2 µL were spotted in ~5 mm distance from each other on a nylon membrane loaded LB_{Kan} agar plate supplemented with 100 µM $PrCl_3$. For comparison, also 3 x 2 µL of PedH as well as EGFP producing cells were spotted on the same membranes. Cell growth, protein production and PQQ-ADH activity screening with 10 mM HMFA as substrate were performed as described above. Subsequently the plasmids were isolated from clones that showed increased activity with 10 mM HMFA in comparison to the PedH reference colonies and submitted for sequencing. The final evaluation of the identified clones was performed using the colorimetric enzyme activity assay with purified enzymes.

Molecular cloning. The gene encoding PedH (PP_2679) was PCR amplified from genomic DNA of *Pseudomonas putida* KT2440 without the signal peptide (PedH28-595) using the following forward primer (5′- ttaaggtctcccatgGCTGTCAGCAATGAAGAAATCCTCCA-3′) and reverse primer (5′-

ttaaggtctcctcgagTTAgtggtgatggtgatgatgTGGCTTGACGCTTGCCG-3′) containing a *NcoI* and *XhoI* restriction site and the coding sequence for a c-terminal hexa-histidine tag. The fragment was digested with *NcoI* and *XhoI* and cloned into pET24d(+) (Novagen) yielding in pET24d-PedH. Mutants have been cloned using Golden Gate Mutagenesis. The mutant fragments were amplified from pET24d-PedH using forward and reverse primers having the desired mutation and BsaI restriction site. All Golden Gate reactions were performed in a total volume of 15 µl. The final reaction volume contained 1-fold concentrated T4 ligase buffer (Promega, Madison, US). Prepared reaction mixtures (ligase buffer, acceptor plasmid, insert(s)) were adjusted to 13.5 µl with ddH2O. In a final step, the corresponding enzymes were quickly added. First, a volume of 0.5 µl of BsaI-HF®v2 (10 units; New England Biolabs, Ipswich, US) and then 1 µl (1-3 units) of T4 ligase (Promega, Madison, US) was added. Golden Gate reactions were carried out by default under following conditions: a) Enzymatic restriction 37 °C (2 min); b) Ligation 16 °C (5 min) [10 passes each] and c) enzyme inactivation: 80 °C (20 min).

Protein production and purification. For initial screening of enzyme activity as well as biotransformation experiments, protein production and purification was performed as described elsewhere.[2] For enzyme kinetics and crystallography protein production and purification was performed as follows. Briefly; constructs were transformed in *E. coli* BL21 (DE3) (Novagen) for overexpression. Cells were grown in lysogeny-broth (LB) medium, supplemented with 1 % lactose and kanamycin (50 mg/l). Cells were incubated at 30 °C overnight under rigorous shaking (180 rpm). Cells were harvested by centrifugation (3,500 x g, 20 min, 4 °C) and resuspended in 20 ml buffer A (20 mM HEPES-Na, pH 8.0, 500 mM NaCl, 20 mM KCl, 20 mM $MgCl_2$, 40 mM imidazole) before lysis in a M-110L Microfluidizer (Microfluidics). The lysate was cleared at 47,850 x g for 20 min at 4 °C and the supernatant was applied onto 5 ml HisTrap FF columns (GE Healthcare) for NiNTA affinity chromatography. After a wash step with 15 column volumes (CV) of buffer A, proteins were eluted with three CV of buffer B (20 mM HEPES-Na, pH 8.0, 500 mM NaCl, 20 mM KCl, 20 mM $MgCl_2$, 500 mM imidazole). Protein eluted fractions were pooled and treated with a final concentration of 100 mM EDTA prior to concentration in Amicon Ultra-10K centrifugal filters to 2.5 ml and further purified by size-exclusion chromatography (SEC). PedH was purified using a HiLoad 26/600 Superdex 200 column (GE Healthcare) equilibrated in buffer SEC (20 mM HEPES-Na, pH 7.5, 500 mM NaCl). Fractions containing PedH were pooled and concentrated for crystallization experiments.

Screening of enzyme activity

Initial enzyme activity measurements were performed in 96-well plates using 10 mM of substrate and 1 – 20 µg/ml enzyme following an established protocol with minor changes.[2] To represent the screening conditions, 5 µM PQQ instead of 1 µM PQQ and 5 µM $PrCl_3$ instead of 1 µM $PrCl_3$ were used.

Enzyme kinetics measurements. To be able to reach saturating substrate concentrations, a modified protocol was used to determine specific enzyme activities for the analysis of kinetic enzyme parameters. Shortly, 1 ml of assay solution containing 20 mM HEPES-Na (pH 8), 500 µM phenazine methosulfate (PMS), 150 µM 2,6-dichlorophenol indophenol (DCPIP), 25 mM imidazole, 50 µM $PrCl_3$, 0.1 mM PQQ, and 0.2 µM of enzyme. Addition of the enzyme to the reaction mixture started the measurement. Enzyme activity was calculated based on the change in OD_{600} within the first minute upon substrate addition. Assays were performed in two ($PedH^{F412V/W561A}$/FFF) or three replicates (PedH/Ethanol, $PedH^{F412V/W561A}$/Ethanol, $PedH^{F412V/W561A}$/HMF, $PedH^{F412V/W561A}$/HMFA) and data are presented as the mean value with error bars representing the corresponding standard deviation. Kinetic parameters were obtained by fitting the enzyme activities at different substrate concentrations to the Michaelis-Menten equation. Kinetic values are presented as mean value with corresponding standard error.

Crystallization and structure determination. Crystallization was performed by the sitting-drop method at 20 °C in 0.5 µl drops consisting of equal parts of protein and precipitation solutions. PedH wild type was co-crystallized at 250 µM concentration with equimolar concentration of PQQ and metal of interest in 0.1 M sodium acetate pH 4.6 and 30 % (w/v) PEG 2000 MME. PedH$^{F412V/W561A}$ was co-crystallized at 250 µM concentration with equimolar concentration of PQQ and metal of interest within 24 h in 0.2 M Lithium sulfate, 0.1 M sodium cacodylate pH = 6.5, 30 % PEG 400. Prior data collection, crystals were flash-frozen in liquid nitrogen employing a cryo-solution that consisted of mother-liquor supplemented with 30 % (v/v) glycerol. Data were collected under cryogenic conditions at the DESY at beamline P14. Data were integrated and scaled with XDS and merged with XSCALE. Structures were determined by molecular replacement with PHASER, manually built in COOT[6], and refined with PHENIX[7]. The structure of the PedH-PQQ-Metal complex was determined by molecular replacement using the crystal structures of ExaA of *Pseudomonas aeruginosa* (PDB-ID: 1FLG) as search models. Figures were prepared with PYMOL.

Biotransformations and compound analysis. Biotransformations were performed as duplicates with 500 µL reaction solution in sealed 1.5 ml reaction vials at 30°C and 180 rpm shaking. The reaction solution contained 100 mM Tris-HCl (pH 8), 5 µM PQQ, 5 µM PrCl3, 150 µM DCPIP, 500 µM PMS, 25 mM Imidazol, 10 mM HMFA (substrate) as well as purified PedH or PedH$^{F412V/W561A}$ protein (c_{end} = 20 µg/ml). Control reactions were performed without protein. In this setup, electrons are transferred from the active site of the enzyme to the electron mediator PMS and eventually to DCPIP, which itself is slowly re-oxidized by oxygen.[8] Probes were incubated in the dark to reduce light-induced decomposition of PMS.[9] Samples were collected at several time points, filtered and stored at -80°C before product analysis. Furan quantification was performed by HPLC analysis using a Beckman System Gold 126 Solvent module with a 168 diode 201 array detector (Beckman Coulter, Brea; USA) and a SUPELCOSIL™ LC-8-DB HPLC column (Supelco, Bellefonte, USA). Column was tempered to 40°C. As eluent, a binary mix of 100% acetonitrile and 20 mM KH_2PO_4 with 1% acetonitrile (adjusted pH = 7.0, degassed) was used at a flow rate of 0.8 mL min^{-1}. Elution started with an increasing gradient of acetonitrile from 0% to 5% within 3.5 minutes. Acetonitrile gradient increased again from 5% to 40% in the next 2.5 minutes. Afterwards the column was flushed with 20 mM KH_2PO_4 with 1% acetonitrile (adjusted pH = 7.0, degassed) for 2 minutes. UV detection was performed at 230 nm. If needed each compound was detected at distinct wavelengths to separate overlapping peak areas. FDCA shows a signal 264 nm, HMFA at 251nm, FFA at 289 nm, 2,5-Bis(hydroxymethyl)furan (HMFOH) at 225 nm and HMF at 285 nm. Retention times of furan compounds were 2.62 minutes, 2.83 minutes and 2.13 minutes for HMFA, FFA and FDCA, respectively. Further compounds HMF and HMFOH had retention times of 5.35 minutes and 4.4 minutes.

Table S1: Composition of the individual screened PedH mutant libraries.

Library	Mutated residues
1	A556 + W561
2	F412 + W561
3	F412 + A556
4	L455 + W561
5	F412 + L455
6	F459 + W561
7	F412 + F459
8	I461 + F412
9	I461 + L455
10	I461 + F459
11	I461 + A556
12	I461 + W561

Table S2: Correlation matrix of active site and substrate channel residues extracted from 3DM-database of PQQ-dependent alcohol dehydrogenases (1 ≙ 100% and 0 ≙ 0% coevolution of two distinct alignment positions in 3DM-database).Combinations of residues that were selected for mutant library generation are colored in red.

Position	W285	F412	L413	L455	F459	I461	A556	W561
W285	-	0.14	0.11	0.19	0.15	0.24	0.18	0.19
F412	0.14	-	0.36	0.77	0.74	0.88	0.92	0.79
L413	0.11	0.36	-	0.32	0.29	0.39	0.36	0.32
L455	0.19	0.77	0.32	-	0.71	0.84	0.84	0.74
F459	0.15	0.74	0.29	0.71	-	0.78	0.76	0.74
I461	0.24	0.88	0.39	0.84	0.78	-	0.93	0.78
A556	0.18	0.92	0.36	0.84	0.76	0.93	-	0.79
W561	0.19	0.79	0.32	0.74	0.74	0.78	0.79	-

Table S3: Crystallographic data collection and refinement statistics for PedH and PedH$^{F412V/W561A}$.

	PedH	**PedH$^{F412V/W561A}$**
Data collection		
Space group	$P4_32_12$	$P4_32_12$
Resolution range (Å)	47.81 - 1.648 (1.707 - 1.648)	47.19 - 1.70 (1.661 - 1.604)
Unit cell parameters		
a, b, c (Å)	105.28, 105.28, 187.13	105.53, 105.53, 186.88
α, β*, γ* (°)	90, 90, 90	90, 90, 90
R_{merge}	0.2083 (3.522)	0.1844 (2.846)
Average $I/\sigma(I)$	14.23 (1.11)	9.57 (0.75)
No. of total reflections	3378794 (330606)	3724161 (366029)
Completeness (%)	99.84 (98.85)	99.79 (98.45)
$CC_{1/2}$(%)	0.999 (0.492)	0.998 (0.322)
Refinement		
R_{work}	0.1473 (0.2669)	0.1538 (0.3257)
R_{free}	0.1592 (0.2833)	0.1687 (0.3432)
No. of atoms		
Overall	5028	9971
Protein	4384	8723
Ligands	26	64
Water	618	1184
Average *B*-factor(Å^2)		
Overall	27.6	25.68
Protein	25.98	24.13
Ligands	19.51	24.28
Water	39.38	37.18
Root-mean-square deviation		
Bond lengths (Å)	0.011	0.011
Bond angles (°)	1.42	1.16
Ramachandran plot (%)		
Favored	95.89	96.15
Allowed	3.57	3.58
Outliers	0.54	0.27

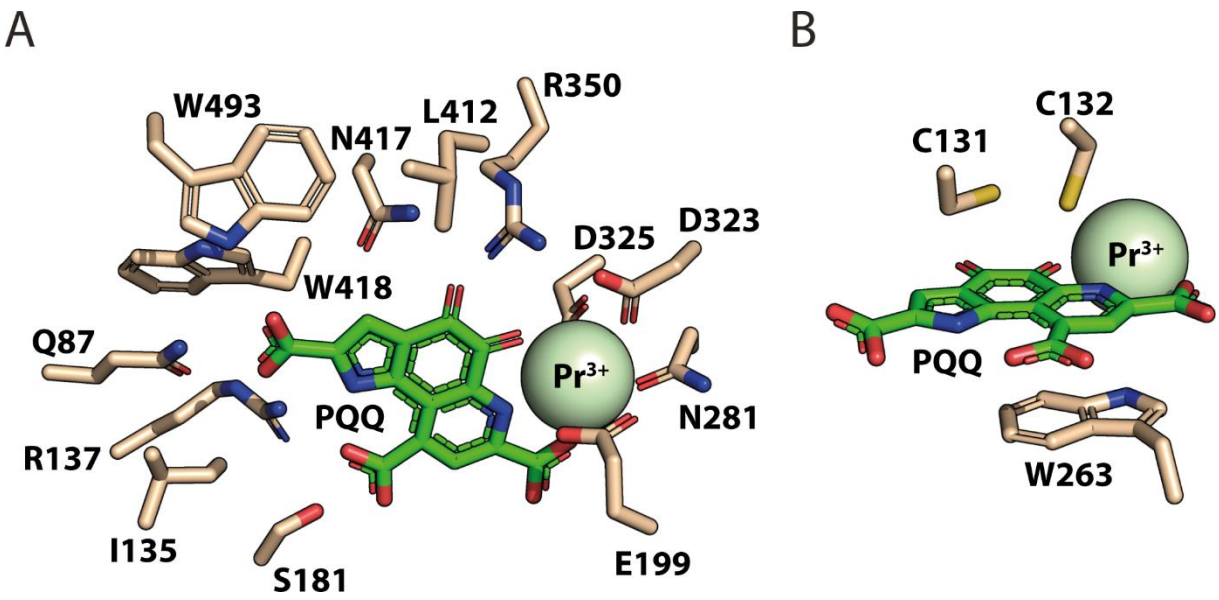

Figure S1: Coordination of PQQ in the active site of PedH. A) Top view depicting residues in the same plane as PQQ and the 4 residues coordinating the metal praseodymium. B) Side view depicting the stacking of PQQ between W263 and the disulfide bridge between C131 and C132**.**

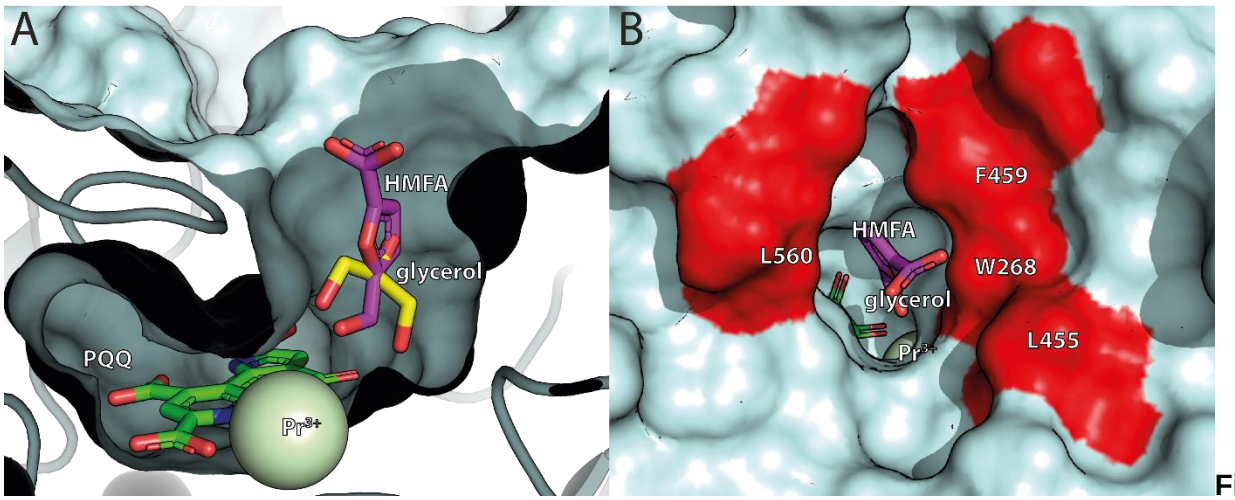

Figure S2: A) Cutaway of the active site of PedH$^{F412V/W561A}$. HMFA (purple) is superimposed onto glycerol (yellow) and would fit into the widened substrate channel of the variant**.** B) Top-view of the active site of PedH$^{F412V/W561A}$ with HMFA (purple) superimposed onto glycerol (yellow). Surface of amino acid residues pointing to the carboxyl group of HM that are not part of the catalytic mechanism are colored in red.

References

(1) Maniatis, T.; Fritsch, E.; Sambrook, J.; Laboratory, C. S. H. *Molecular Cloning : A Laboratory Manual*; Cold Spring Harbor, N.Y. Cold Spring Harbor Laboratory, 1982.

(2) Wehrmann, M.; Billard, P.; Martin-Meriadec, A.; Zegeye, A.; Klebensberger, J. Functional Role of Lanthanides in Enzymatic Activity and Transcriptional Regulation of Pyrroloquinoline Quinone-Dependent Alcohol Dehydrogenases in Pseudomonas Putida KT2440. *MBio* **2017**, *8* (3), e00570-17. https://doi.org/10.1128/mBio.00570-17.

(3) Gibson, D. G. Enzymatic Assembly of Overlapping DNA Fragments. *Methods Enzymol.* **2011**, *498*, 349–361. https://doi.org/10.1016/B978-0-12-385120-8.00015-2.

(4) Wehrmann, M.; Klebensberger, J. Engineering Thermal Stability and Solvent Tolerance of the Soluble Quinoprotein PedE from Pseudomonas Putida KT2440 with a Heterologous Whole-Cell Screening Approach. *Microb. Biotechnol.* **2018**, *11* (2), 399–408. https://doi.org/10.1111/1751-7915.13036.

(5) Reetz, M. T.; Kahakeaw, D.; Lohmer, R. Addressing the Numbers Problem in Directed Evolution. *ChemBioChem* **2008**, *9* (11), 1797–1804. https://doi.org/10.1002/cbic.200800298.

(6) Emsley, P.; Cowtan, K. Coot: Model-Building Tools for Molecular Graphics. *Acta Crystallogr. D. Biol. Crystallogr.* **2004**, *60* (Pt 12 Pt 1), 2126–2132. https://doi.org/10.1107/S0907444904019158.

(7) Adams, P. D.; Afonine, P. V; Bunkóczi, G.; Chen, V. B.; Davis, I. W.; Echols, N.; Headd, J. J.; Hung, L.-W.; Kapral, G. J.; Grosse-Kunstleve, R. W.; McCoy, A. J.; Moriarty, N. W.; Oeffner, R.; Read, R. J.; Richardson, D. C.; Richardson, J. S.; Terwilliger, T. C.; Zwart, P. H. PHENIX: A Comprehensive Python-Based System for Macromolecular Structure Solution. *Acta Crystallogr. D. Biol. Crystallogr.* **2010**, *66* (Pt 2), 213–221. https://doi.org/10.1107/S0907444909052925.

(8) Naumann, R.; Mayer, D.; Bannasch, P. Voltammetric Measurements of the Kinetics of Enzymatic Reduction of 2,6-Dichlorophenolindophenol in Normal and Neoplastic Hepatocytes Using Glucose as Substrate. *Biochim. Biophys. Acta - Mol. Cell Res.* **1985**, *847* (1), 96–100. https://doi.org/10.1016/0167-4889(85)90158-2.

(9) Jahn, B.; Jonasson, N. S. W.; Hu, H.; Singer, H.; Pol, A.; Good, N. M.; Op den Camp, H. J. M.; Cecilia, D. C. N.; Gomez, M.; Daumann, L. Understanding the Chemistry of the Artificial Electron Acceptors PES , PMS , DCPIP and Wurster ' s Blue in Methanol Dehydrogenase Assays. *JBIC J. Biol. Inorg. Chem.* **2020**, No. 0123456789. https://doi.org/10.1007/s00775-020-01752-9.